Neural interfacing architecture enables enhanced motor control and residual limb functionality postamputation

Shriya S. Srinivasan[a,b,c,1], Samantha Gutierrez-Arango[a], Ashley Chia-En Teng[d], Erica Israel[a], Hyungeun Song[a,b], Zachary Keith Bailey[a,e], Matthew J. Carty[a,f,c], Lisa E. Freed[a,b], and Hugh M. Herr[a,c,1]

[a]MIT Center for Extreme Bionics, Biomechatronics Group, Massachusetts Institute of Technology, Cambridge, MA 02139; [b]Harvard-MIT Program in Health Sciences and Technology, Massachusetts Institute of Technology, Cambridge, MA 02139; [c]Harvard Medical School, Boston, MA 02114; [d]Department of Mechanical Engineering, Massachusetts Institute of Technology, Cambridge, MA 02139; [e]Department of Mechanical Engineering, United States Air Force Academy, Colorado Springs, CO 80920; and [f]Division of Plastics and Reconstructive Surgery, Brigham and Women's Hospital, Boston, MA 02114

Edited by Peter L. Strick, University of Pittsburgh, Pittsburgh, PA, and approved December 30, 2020 (received for review September 16, 2020)

Despite advancements in prosthetic technologies, patients with amputation today suffer great diminution in mobility and quality of life. We have developed a modified below-knee amputation (BKA) procedure that incorporates agonist–antagonist myoneural interfaces (AMIs), which surgically preserve and couple agonist–antagonist muscle pairs for the subtalar and ankle joints. AMIs are designed to restore physiological neuromuscular dynamics, enable bidirectional neural signaling, and offer greater neuroprosthetic controllability compared to traditional amputation techniques. In this prospective, nonrandomized, unmasked study design, 15 subjects with AMI below-knee amputation (AB) were matched with 7 subjects who underwent a traditional below-knee amputation (TB). AB subjects demonstrated significantly greater control of their residual limb musculature, production of more differentiable efferent control signals, and greater precision of movement compared to TB subjects ($P < 0.008$). This may be due to the presence of greater proprioceptive inputs facilitated by the significantly higher fascicle strains resulting from coordinated muscle excursion in AB subjects ($P < 0.05$). AB subjects reported significantly greater phantom range of motion postamputation (AB: 12.47 ± 2.41, TB: 10.14 ± 1.45 degrees) when compared to TB subjects ($P < 0.05$). Furthermore, AB subjects also reported less pain (12.25 ± 5.37) than TB subjects (17.29 ± 10.22) and a significant reduction when compared to their preoperative baseline ($P < 0.05$). Compared with traditional amputation, the construction of AMIs during amputation confers the benefits of enhanced physiological neuromuscular dynamics, proprioception, and phantom limb perception. Subjects' activation of the AMIs produces more differentiable electromyography (EMG) for myoelectric prosthesis control and demonstrates more positive clinical outcomes.

neural engineering | amputation | physiology | sensory feedback | prosthetics

The standard-of-care surgical approach to amputation has not seen considerable innovation since its conception in the mid-1800s (1), despite significant progress in biomechatronics and advanced reconstructive techniques. The typical amputation procedure neglects neurological substrates and disrupts key neuromuscular relationships responsible for bidirectional (efferent, afferent) signaling. The deafferentation of lower motor neurons triggers central reorganization of motor circuits, which negatively impacts motor imagery and motor coordination (2, 3) and results in significant neuroma pain (4–6), phantom pain (7), and maladaptive or diminishing phantom sensation (8–10). Phantom sensation, the perception of one's phantom limb while at rest and in motion, is an important component of motor imagery utilized in the preparation of motor control commands and can be a source of chronic irritation, if unpleasant. The haphazard arrangement and myodesis of residual musculature further constrain the ability for individual muscles to dynamically excurse, causing cocontraction of muscles and changing gait patterns (11–14). Together, these peripheral and central modifications result in the poor production of efferent signals for direct myoelectric control (15, 16). To compensate for these shortcomings, considerable effort has been spent on developing and deploying pattern-recognition–based myoelectric control strategies (17–19). However, even with these advanced myoelectric devices and controllers, end users find their operation cumbersome and time consuming (20). Motor control is also challenged by the lack of proprioceptive sensory feedback from prostheses (12, 21–23). Together, the limitations of the current amputation approaches significantly lower the quality of life for persons with amputation (24–27).

In recognition of these shortcomings, surgical researchers have recently begun to explore new strategies to modify standard amputation procedures. Targeted muscle reinnervation (TMR) (28, 29) and regenerative peripheral nerve interfaces (RPNIs) (30, 31) represent approaches that are designed to provide greater efferent motor signals for myoelectric control and mitigate neuroma pain. However, neither approach offers muscle–tendon afferent

Significance

Despite advancements in prosthetic technologies, persons with amputation today suffer great diminution in mobility and quality of life. This is largely due to an outdated amputation paradigm that precludes efficacious communication between the residual limb and prosthesis. An amputation method utilizing agonist–antagonist myoneural interfaces (AMIs) constructs neuromuscular substrates in the residual limb to avail enhanced sensorimotor signaling. In our study, subjects with AMI amputation demonstrate improved motor control, phantom sensations, range of motion, and decreased pain when compared to patients with traditional amputation. With the demonstrated increases in motor coordination and position differentiation, our results suggest that patients with AMI amputation will be able to more efficaciously control bionic prostheses.

Author contributions: S.S.S., M.J.C., and H.M.H. designed research; S.S.S., S.G.-A., E.I., H.S., Z.K.B., M.J.C., and L.E.F. performed research; S.S.S., S.G.-A., A.C.-E.T., E.I., Z.K.B., M.J.C., and L.E.F. analyzed data; and S.S.S., M.J.C., L.E.F., and H.M.H. wrote the paper.

Competing interest statement: H.M.H., M.J.C., and S.S.S. hold a patent related to AMI surgical amputation procedures.

This article is a PNAS Direct Submission.

[1]To whom correspondence may be addressed. Email: shriyas@mit.edu or hherr@media.mit.edu.

This article contains supporting information online at https://www.pnas.org/lookup/suppl/doi:10.1073/pnas.2019555118/-/DCSupplemental.

Published February 15, 2021.

proprioceptive signaling, which is physiologically mediated by agonist–antagonist muscle dynamics and critical for trajectory planning, fine motor control, and reflexes (32, 33).

The agonist–antagonist myoneural interface (AMI) is a more recent surgical approach and neural interfacing strategy designed to augment volitional motor control and restore muscle–tendon proprioception (11, 12, 34–37) by surgically coapting agonist and antagonist muscles to restore natural physiological muscle pairing and dynamics. When the agonist muscle contracts, the antagonist muscle stretches (or vice versa), giving rise to musculotendinous afferent feedback from muscle spindle fibers (length and velocity) and Golgi tendon organs (force). For each joint in a bionic limb, one AMI is surgically constructed in the residuum. Functional electrical stimulation (FES) applied to the antagonist muscle of the AMI can provide force or position feedback onto the agonist (or vice versa) from a bionic prosthesis to inform the user of prosthetic torque or position, respectively (11). In Clites et al. (11), an early human subject with an AMI amputation demonstrated dynamic muscle excursions, individualized contraction of each AMI muscle, and graded proprioceptive muscle–tendon feedback in response to muscle activation. This subject additionally demonstrated greater control of joint position, impedance, and FES-based torque feedback from a bionic prosthesis when compared to subjects with a traditional amputation. This pilot study demonstrated the potential of the AMI and paved the way for further implementation and investigation of the physiological properties, phantom limb perceptions, pain, and motor control of the AMI neuromuscular constructs.

In this study, we characterize the physiological outcomes of subjects with an AMI below-knee amputation (AB) ($n = 15$) and compare them against those of matched control subjects with a traditional below-knee amputation (TB) ($n = 7$). Given the emphasis placed on the reconstruction of peripheral neuromusculature with AMIs, we hypothesize that the AB cohort will experience an enhancement in phantom sensation and range of motion (ROM) percepts compared with the TB cohort. As a result of the dynamically coupled agonist–antagonist muscles comprising the AMI constructs, we also hypothesize that the AB cohort will demonstrate greater muscle excursion and fascicle strains compared to the TB population. With these improvements in residual limb muscle dynamics, motor capabilities, and perception, we further anticipate that AB subjects will demonstrate greater accuracy and precision of performance on ankle and subtalar intended movements compared to matched TB participants. These hypotheses are evaluated through a combination of electromyography (EMG), goniometry, ultrasonography, and surveys.

Methods

Study Design. The study was conducted at the Massachusetts Institute of Technology (MIT) Biomechatronics Group in Cambridge, MA, between March 2017 and March 2020 under approval of NCT03374319 (https://www.clinicaltrials.gov/) and MIT's Committee on the Use of Humans as Experimental Subjects (protocol 1801183130). Twenty-two individuals with unilateral transtibial amputations were consented. Fifteen subjects had undergone a unilateral below-knee amputation incorporating AMIs (AB cohort) at the Brigham and Women's Hospital. Seven subjects with traditional below-knee amputation served as controls (TB cohort). All subjects had undergone standard physical therapy directed toward achieving a normal gait pattern.

Participants. Participants were eligible if they were between 18 and 65 y of age, had a fully healed residuum, and were active users of a standard prosthesis with an ability for ambulation with variable cadence. Exclusion criteria included cardiopulmonary instability manifest as coronary artery disease and/or chronic obstructive pulmonary disease, extensive peripheral neuropathy, and extensive microvascular compromise.

The study design allowed for the control group to represent a range of below-knee amputation (BKA) techniques, together representing the "standard amputation." As such, subjects had undergone standard amputations by vascular and orthopedic surgeons, the traditional services performing amputations. One TB subject had undergone targeted muscle reinnervation (38), and another had undergone an osteomyoplastic "Ertl" amputation (39, 40), techniques not specifically aimed at restoring musculotendinous proprioceptive feedback. Since our outcome measures were largely targeted on aspects influenced by musculotendinous proprioception, we grouped these subjects in the TB category.

Randomization and Blinding. Participant allocation was nonrandomized, and the study was not blinded as the AB cohort was drawn from a pool of patients who had previously undergone the AMI BKA procedure at the Brigham and Women's Hospital (under NCT03374319) by Matthew Carty. Willingness to enroll in complementary functional outcomes testing at MIT was included as an eligibility criterion for enrollment in the Brigham and Women's Hospital trial. Each subject in the TB cohort was prospectively matched to a subject within the AMI group to the degree possible based on age and time since amputation.

Interventions. Participants in the AB cohort had received two surgically constructed AMIs in their residuum during their amputation according to the method described in ref. 12 (Fig. 1*A*). Briefly, AMIs were constructed for the ankle and subtalar joints; the tibialis anterior (TA) and lateral gastrocnemius (LG) were coapted through a synovial tunnel anchored on the medial flat of the tibia to form the ankle AMI. The peroneus longus (PL) and tibialis posterior (TP) were utilized similarly for the subtalar joint. The synovial canals as well as embedded tendons were harvested from the lateral or medial malleoli in the discarded ankle. Two tantalum bead markers (Halifax Biomedical Inc.; Halifax Bead Set, 1 mm) were inserted into each muscle and one in each synovial tunnel to enable noninvasive monitoring of the muscle dynamics postoperatively. RPNIs were created for any transected sensory, cutaneous, and motor nerves encountered during surgery.

Each participant within the TB group received a traditional BKA without surgically reconstructed AMIs.

Outcomes. Testing in the AB cohort was categorized into "short term" (6 to 12 mo postoperatively) and "long term" (12+ mo) time frames to capture changes that occurred as neuromuscular constructs underwent remodeling. All AB subjects were tested once within the short-term frame and six AB subjects underwent additional testing in the long-term frame. Two subjects (AB 30 and TB 22) were unable to complete the EMG- and ultrasound-based testing due to logistical challenges.

Pain Score. The Patient-Reported Outcomes Measurement Information System (PROMIS) Sleep Disturbance 6a tool and Pain Interference 6a survey (41) were administered to all AB subjects at the following time points: preoperatively and 3, 6, 9, 12, and 24 mo postoperatively. During their testing session at the Biomechatronics laboratory, both TB and AB subjects were administered the same survey orally.

Phantom Limb Sensation. Using open-ended questions, subjects were asked to describe their phantom limb percepts during walking, as well as during rest with the prosthesis worn and with the prosthesis not worn. Subjects were then specifically asked to relate the level of perception of their lateral and medial malleoli, heel pad, arch of the foot, balls of the footpad, and toes. The more thorough and tangible the phantom limb felt to subjects, the greater the phantom sensation scored. Responses were independently graded on a 1 to 3 scale and compared between cohorts using a Student's *t* test, as the data satisfied requirements for normality and variance in each cohort.

Characterization of Muscle Activation Using EMG. Bony anatomical landmarks and target muscles were identified by palpation and their superficial projections were marked using a skin marker and reflective balls (*SI Appendix*, Fig. S1 *A*–*C*). Surface EMG electrodes were placed on the affected and unaffected limbs (*SI Appendix*, Fig. S1 *D* and *E*), focusing on the muscle regions. Initially, the EMG data were collected using eight wireless bipolar electrodes (Trigno; Delsys) overlying the LG, TA, TP, and PL muscles sampled at 1,200 Hz. Starting in June 2019 we utilized up to 128 H124SG Ag/AgCl electrodes (Covidien), sampled at 2,048 Hz (Twente Medical Systems International [TMSi] Refa136; Type Refa_Ext-128e4b4a; REF code 95-0121-6446-1). Transparent plastic strips, with electrodes positioned at ∼2.5-cm intervals, aided in the placement and alignment of electrodes in a grid-like fashion (*SI Appendix*, Fig. S1 *D* and *E*). On the unaffected limb, electrodes were positioned over the native anatomical locations of the muscles incorporated in the AMI. Raw EMG was high-pass filtered at 70 Hz, full-wave rectified, and integrated using a 100-ms moving average window to obtain the muscle activation (12).

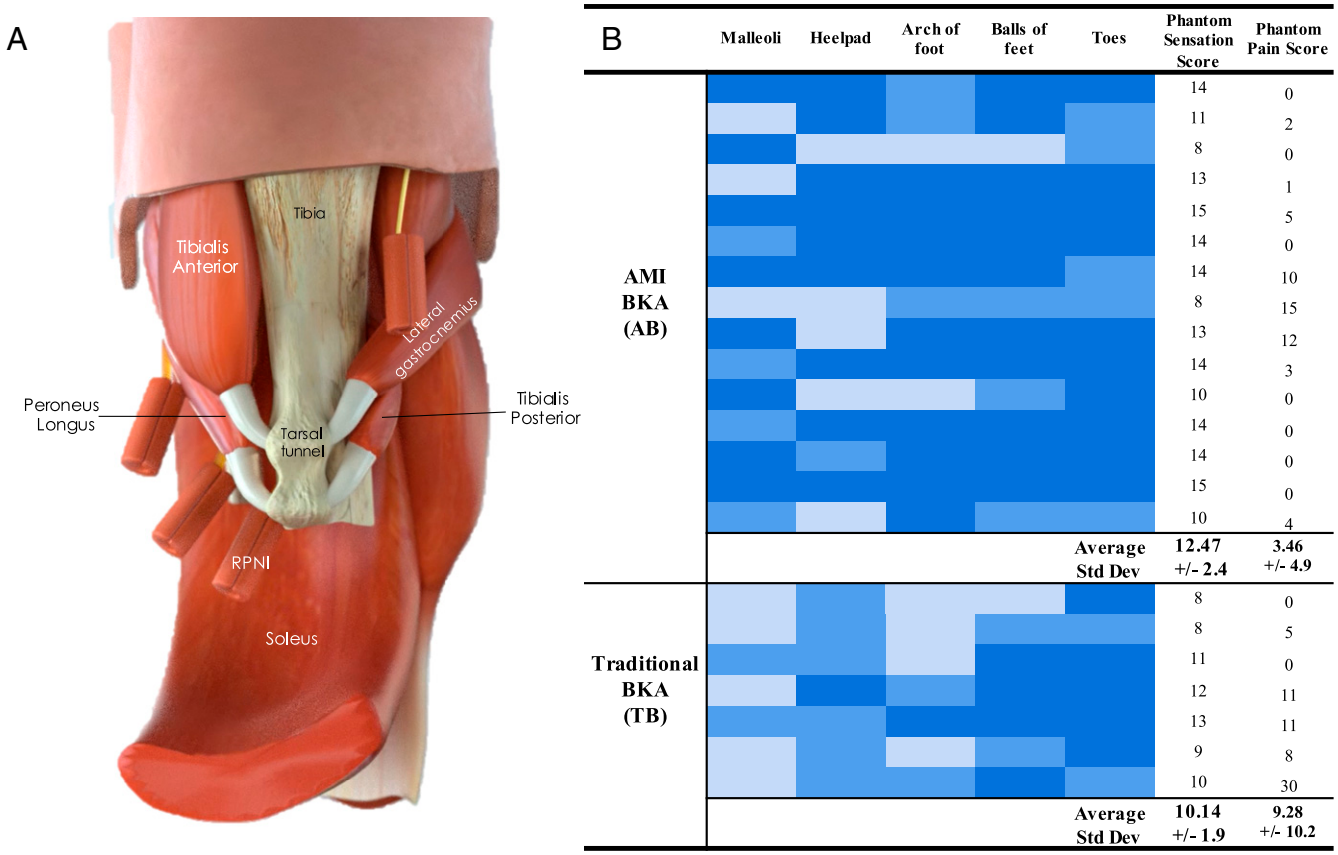

Fig. 1. (*A*) Illustration of the AMI constructs in the residuum of a BKA. The TA and LG form the ankle AMI through coaptation to the tendon in the tarsal (synovial) tunnel anchored on the tibia. The TP and PL form the subtalar AMI and pass through a more distal tarsal tunnel. These AMIs are positioned superficially to enable strong and independent EMG control signals for a myoelectric prosthesis. RPNIs are created for transected cutaneous, sensory, and motor nerves for neuroma prophylaxis. Positioning of these elements is representative and not to scale. (*B*) Phantom sensation and pain scores are listed for each subject. Phantom sensation for each part of the leg is represented colorimetrically (dark blue, very vivid; light blue, less perceptible). Phantom sensations in the AB cohort ($n = 15$) are significantly greater than those in the TB cohort ($n = 7$) ($P < 0.05$, Student's t test). Pain scores are considerably lower in the AB cohort compared to the TB cohort ($n = 7$, $P = 0.08$, Student's t test).

The optimal electrode placement for each muscle was selected using a semiautomated process, thresholding for the highest signal-to-noise ratios during composite movements.

Synchronous Measurement of Intended Phantom Movements. Subjects were asked to recline in a supine position with their intact limb positioned on a trapezoidal foam riser pillow to allow free movement of the ankle while minimizing motion of the electrodes and wiring (*SI Appendix*, Fig. S2). A 2 degrees-of-freedom wireless goniometer (Bio-Metrics Ltd.; WS200 DataLITE 2 Goniometer system with W110-Ankle and W150-Knee, and DataLITE Management Software 51025-00) was secured to the posterior aspect of the unaffected leg (*SI Appendix*, Fig. S2*A*) and used to synchronously measure ankle–foot kinematics for the unaffected limb. For all tasks, subjects were asked to mirror phantom movements onto the contralateral foot. Time-synchronized EMG and goniometry data were simultaneously recorded for all tasks to provide a one-to-one temporospatial indicator of the efferent signaling and intended joint movement of the phantom limb.

Study of Muscle Coupling and Excursion, Fascicle Strain, and AMI Construct Morphology. Muscle dynamics, tissue remodeling, scarring, and tantalum bead movement were assessed using a portable high-definition ultrasound scanner at 60 fps (LS128; Telemed) during volitional activation of the AMI muscles (*SI Appendix*, Fig. S3). First, subjects were instructed to plantarflex (PF) and dorsiflex (DF) the phantom ankle joint while recording ultrasound from the tibialis anterior. Then, ultrasound of the tibialis posterior was recorded during inversion (IN) and eversion (EV) of the phantom subtalar joint. EMG and ultrasound measurements were analyzed to characterize muscle coupling. Imaging of the synovial tunnels was performed to quantify movement of the AMI construct through the synovial tunnel and surveil for dehiscence or scarring. Ultrasonographic planes capturing tantalum bead markers or their artifacts were prioritized to allow for quantitative measurements of fascicle strain. In cases where the beads were not visualized in AB subjects and for all TB subjects, fascicle lengths were identified, tracked, and measured using the UltraTrack v2 MATLAB (R_2018a) package (42). In control subjects, the most closely related and palpable muscle mass associated with each movement was used as a proxy if the original target muscle was unavailable (12).

ROM Percepts. Subjects were asked to demonstrate and mirror the ROM possible of the affected or phantom joints on their unaffected limb, pre- and postoperatively at least three times. The angles of PF and DF were measured using the Biometrics 2-axis goniometer attached to the ankle region and averaged across trials. Data were processed through custom scripts in MATLAB (Mathworks) to identify the maximum amplitude for each movement and normalized as a percentage of the amplitude of the contralateral limb.

Motor Control Performance Tasks. Subjects were then asked to perform PF, DF, IN, and EV of the ankle and subtalar joints, respectively, for 20 repetitions each at three different speeds. Subjects were then asked to rotate the foot and ankle in clockwise and counterclockwise circles. Commands were presented through an audio recording to ensure consistency across trials and subjects. Prior to these trials, subjects were educated on the isolation of each movement and were encouraged to focus on moving the joint to a given

position, rather than activating the muscles. Tasks were performed without visual feedback to force subjects to use proprioception to close the loop on their internal efferent–afferent neuromuscular physiology.

A positional differentiation task was created to determine the ability of subjects to produce phantom movements with precision in position and muscle activation level. Subjects were instructed to move their limb to 0, 25, 50, 75, and 100% of their full ROM for PF and DF. Subjects were instructed to move the subtalar joint to 50 and 100% of their ROM for inversion and eversion. Only two levels were assessed for inversion and eversion as the subtalar joint range of motion was relatively limited, compared to the ankle, constraining goniometer-based classification of activation level. Commands for the ankle and subtalar movements were presented 40 and 30 times, respectively, and in random order to each subject through a custom MATLAB script displayed on a screen (*SI Appendix*, Fig. S2). This task assayed the proprioceptive feedback received and incorporated into each subject's motor control; subjects with greater proprioception would be able to better determine the position of the joint and thus more precisely execute the task at each gradation. The muscle activation level was quantified by the EMG signal amplitude at each commanded movement, as identified through time-synched EMG and commands. The control of movements and distinctness of the efferent signals were compared between cohorts using a heteroscedastic two-tailed test on the means between adjacent activation levels at $P < 0.05$. The variance of performance was compared using a repeated-measures F test at $P < 0.05$, Bonferroni corrected for multiple comparisons at a statistical significance alpha of $P < 0.008$.

Statistical Analysis. MATLAB (Mathworks) was used for all data and statistical analyses. Data distribution was assumed to be normal, but was not formally tested. For temporal correlations, data were normalized to the maximal amplitude of each subject for EMG, fascicle strain, and joint angle to allow for uniform comparisons across subjects and groups. All data are reported as mean ± SD and unless otherwise noted, heteroscedastic two-tailed Student's t tests were used to compare differences between groups with an alpha of $P < 0.05$.

Results

Subject Demographics. The study population and demographic data for the 15 AB subjects and 7 TB subjects studied are presented in Table 1. A subset of the AB cohort was matched by age and time since amputation in the TB cohort. The mean ages at the time of surgery were 39.0 ± 12.1 y old for the AB cohort and 45.5 ± 16.9 y old for the TB cohort. Trauma was the primary etiology for the majority of subjects. Subjects were well matched between the AB and TB cohorts and individual TB-AB subject matches. No significant difference in ages or time since amputation were present (Student's t test, $P < 0.05$). Nine of 15 (60%) subjects in the AB cohort and 3/7 (43%) subjects in the TB cohort were male. All subjects underwent standard physical therapy directed toward achieving a normal gait pattern. Representative videos of AMI construct motion within the residuum are presented in Movie S1, exhibiting the nature of the muscle movement and tissue remodeling in the residuum at 6 and 22 mo.

Phantom Sensations and Pain. Phantom sensations, the perceptible features of one's phantom joint, and phantom pain levels were surveyed (Fig. 1*B*). AB subjects reported significantly higher phantom sensations (12.47 ± 2.41, $P = 0.03$) compared to TB subjects (10.14 ± 1.9) ($P < 0.05$, Student's t test). AB subjects reported on average less pain (12.25 ± 4.9) as compared to the TB cohort (17.29 ± 10.22) ($P = 0.08$, Student's t test). Notably, 6 of the 15 subjects in the AB cohort indicated zero pain in all categories. Notably, within the AB cohort, a comparison of pain scores between their preoperative baseline and postoperative levels at 3, 6, 9, 12, and 24 mo demonstrated significant decreases (*SI Appendix*, Fig. S4, $P < 0.005$, Student's t test).

In self-reported responses to a survey of residuum movements and perception, over half of AB subjects indicated that they "move their AMIs passively" during the day for construct mobilization. Additionally, 60% of AB subjects reported that they fired the AMI muscles during walking with a standard prosthesis. For many, this was not a conscious movement, while for others, physical therapy and focused effort enabled this motion. In contrast, TB subjects predominantly reported that they fired the calf muscle with the intent of "holding up the socket." When asked to describe the sensation of the phantom limb, AB subjects stated a range of observations. Some indicated that their phantom "felt like the normal limb,, while others noted that "I can wiggle my toes, especially my big toe." One AMI subject indicated that the toes were uncomfortably constrained or "wrapped in a towel" in the residuum. This sensation was reduced after this subject received a soft tissue revision which addressed issues related to poor wound healing during the initial amputation. The revision may have enabled the AMIs to move with greater ease.

Coupled Motion and Muscle Excursion. Ultrasound imaging demonstrated coupled agonist–antagonist motions within each ankle and subtalar AMI; as the agonist contracted, the antagonist muscle underwent dramatic stretch and sliding (Movie S2). With the exception of the TB 20, who had undergone an Ertl osteomyoplastic amputation, dynamic coupling of antagonistic muscles was not present in TB subjects (Movie S3). During cycled phantom joint movements, we additionally visualized the synovial tunnels to see coordinated sliding of the subtalar and ankle AMIs (Movies S4 and S5 and *SI Appendix*, Fig. S3). No dehiscence of constructs was witnessed in any AB subjects. However, in some TB subjects, excessive scarring between muscles and soft tissue significantly barred muscle motions. This imaging evidenced the desired functioning of the agonist–antagonist mechanism which generates afferent spindle feedback through changes in muscle length and Golgi tendon feedback through changes in muscle force.

To quantify changes in muscle length, the fascicle strains from the antagonist muscle were measured during agonist contraction. Significantly greater fascicle strains were produced in ABs compared to TBs (Fig. 2*A*, $P < 0.05$, Student's t test). Because these excursions can be constrained by tissue remodeling, scarring, or muscle atrophy, we compared the mean fascicle strains produced by AB subjects between their first and second testing sessions and found no significant changes (Fig. 2*B*, $P > 0.05$, Student's t test). Similarly, no changes were detected in ultrasound imaging capturing the AMI muscles sliding through the synovial tunnels. These measurements indicate the chronic stability of the AMI mechanism and the ability for the synovial tunnels to provide a lubricious sliding surface (measurements taken out to 33 mo postoperatively).

ROM Percepts. Prior to amputation, many subjects had suffered traumatic injuries or surgical interventions (such as joint fusion) that "locked" or restricted the ROM of their joints, a source of considerable pain and discomfort. Because the AMI amputation mobilizes muscles and enables them to excurse within the residuum, ABs were expected to achieve greater muscle movements than previously possible with their preamputation etiologies. We thus investigated the effect of these dynamic excursions on the ROM percepts, which are known to guide motor imagery and prosthetic control. The demonstrated ROM of the phantom limb in each direction (PF, DF, IN, EV) were normalized as a percentage of the unaffected joints' ROM (Fig. 2*C*). The mean and distributions of preamputation ROM percepts for AB and TB cohorts were comparable and below 50% of the available ROM accessible to the unaffected limb, in all directions. In a comparison of pre- and postamputation ROM percepts, AB subjects experienced significant increases in the PF, EV, and DF ($P < 0.05$, Student's two-tailed t test) directions. In contrast, an improvement in ROM percepts following amputation was not detected in the TB cohort. Further, AB subjects experienced significantly greater ROM than TB subjects following amputation for PF, DF, and EV ($P < 0.05$, Student's two-tailed t test). Anecdotally, some subjects made statements such as "my foot feels free, it can finally move."

Table 1. Two cohorts of participants who had previously received below-knee amputations—AMI BKA (AB, $n = 15$) and traditional BKA (TB, $n = 7$)—and participated in evaluations at the Biomechatronics Group within the MIT Media Lab between March 2017 and January 2020

Group	Subject no.	Matched subject no.	Age at surgery (y)	Age at study session (y)	Sex	Laterality	Etiology
AMI BKA (AB)	1	22	41.6	42.6	F	L	Thermal injury
	2	17	52.3	52.9	M	R	Trauma
	3		20.9	21.4	F	L	Iatrogenic
	6	23	49.8	50.5	F	L	Trauma
	7	4	28.2	28.8	F	R	Trauma
	8	10	52.6	54.3	M	L	Trauma
	9	16	25.9	26.4	M	L	Trauma
	11		41.4	41.9	M	L	Vascular
	12		49.2	49.8	F	L	Trauma
	13	20	57.1	57.7	M	R	Trauma
	19		31.8	32.3	M	R	Trauma
	24		22.6	23.2	F	L	Trauma
	25		47.4	47.9	M	R	Trauma
	26		28.4	29.1	M	R	Trauma
	30		36.4	37.9	M	L	Malformity
Mean ± SD			39.0 ± 12.1	39.6 ± 12.6			
Range (y)			21 to 57	21 to 58			
Traditional BKA (TB)	4	7	23.9	25.4	F	R	Oncology
	10	8	59.3	62.0	F	R	Trauma
	16	9	23.3	25.3	M	L	Malformity
	17	2	58.3	59.5	F	L	Trauma
	20	13	59.1	61.9	M	R	Trauma
	22	1	36.7	39.2	M	R	Trauma
	23	6	58.0	60.0	M	L	Trauma
Mean ± SD			45.5 ± 16.9	47.5 ± 17.0			
Range (y)			23 to 59	25 to 62			

Participants' ages at the time of surgery and at their first testing session are provided. Six AB subjects, 1, 2, 3, 7, and 13, underwent testing after 12 mo postoperative as part of a longer-term follow-up. F, female; M, male; L, left; R, right.

Coordination of Movement. With traditional amputation, anatomical reorganization and peripheral deafferentation prompt central reorganization of motor circuits, yielding changes in motor imagery and coordination. With the reinstatement of proprioceptive afferents that guide motor imagery and execution in the AMI amputation, we sought to characterize the coordination between the intended phantom movement (joint angle) and the executed muscle activations (fascicle strains and EMG) in an effort to identify potential effects of reorganization. We found that muscle activation (EMG) was significantly temporally correlated to fascicle strains and intended phantom joint movement in AB subjects ($r^2 > 0.75$, linear regression, Fig. 2 *D* and *E*). In contrast, such temporal correlation of muscle activity to intended phantom movement was not present in most TB subjects (Fig. 2 *F* and *G* and Movie S5). In the TB cohort, correlation coefficients for linear regressions between fascicle strains and EMG ranged between 0.19 and 0.76. Given the isometric nature of the residual muscles and lack of agonist–antagonistic coupling, the muscles' force can oscillate periodically with continued invariance in strain.

Since spindle fibers fire at a rate proportional to the muscle length, the magnitude of fascicle strain serves as an indicator of the resolution of the proprioceptive information possible. Perceptions of the ROM and phantom sensation (PS) are derived from motor imagery pathways incorporating this proprioception. Thus, we assessed the relationship between fascicle strain and ROM or PS to validate these mechanistic links. The relationship between fascicle strain and ROM in the AB and TB cohorts was described by a logarithmic fit for PF ($r = 0.59$) as well as for DF ($r = 0.74$) (*SI Appendix*, Fig. S5 *A* and *B*). In addition, a moderate relationship between fascicle strain and PS was present in the AB cohort, but not in the TB cohort (*SI Appendix*, Fig. S5 *C* and *D*). These findings align with the operational principle of the agonist–antagonist muscle coupling and production of proprioceptive sensations. Of note, two AMI subjects specifically mentioned that their phantom joint would "get stuck" toward the extremes of ankle DF and PF. Ultrasound imaging in these subjects specifically demonstrated that the corresponding muscle bulk under strong contraction was much larger in cross-sectional area than that which could traverse through the synovial canal. These two subjects reported the lowest ranges of motion and their fascicle strains were the lowest two values in the cohort.

Positional Discrimination Task. In a positional differentiation task, subjects were instructed to move their phantom to 0, 25, 50, 75, and 100% of the ROM for each joint. The independence of muscle activation levels, measured by EMG, characterized the subjects' fine motor control and the variance of the activation levels lent insight into their proprioceptive capabilities. Subjects with greater control and proprioception would be able to position their phantom more distinctly and with greater precision. The distinctness of EMG for each muscle activation level is important for determining one's capability for direct myoelectric control of a prosthesis. Boxplots of the EMG activation levels from the median performer in the AB and TB cohorts are presented in Fig. 3 *A* and *B*, respectively, as a representative example. As visualized in Fig. 3 *A* and *B*, greater separation between bars indicates greater positional discrimination. Conversely, for example, in the case of the median TB performer, no differentiation of motor intent for inversion or eversion (50 or 100%) can be derived based on their muscle activation.

An analysis of variance (ANOVA) across all subjects in the two cohorts demonstrated a significant difference between groups ($P < 0.05$, ANOVA). Post hoc analyses of the activation level between adjacent positions (for example, DF 25% vs. DF 50%) demonstrated that AB subjects have more significant

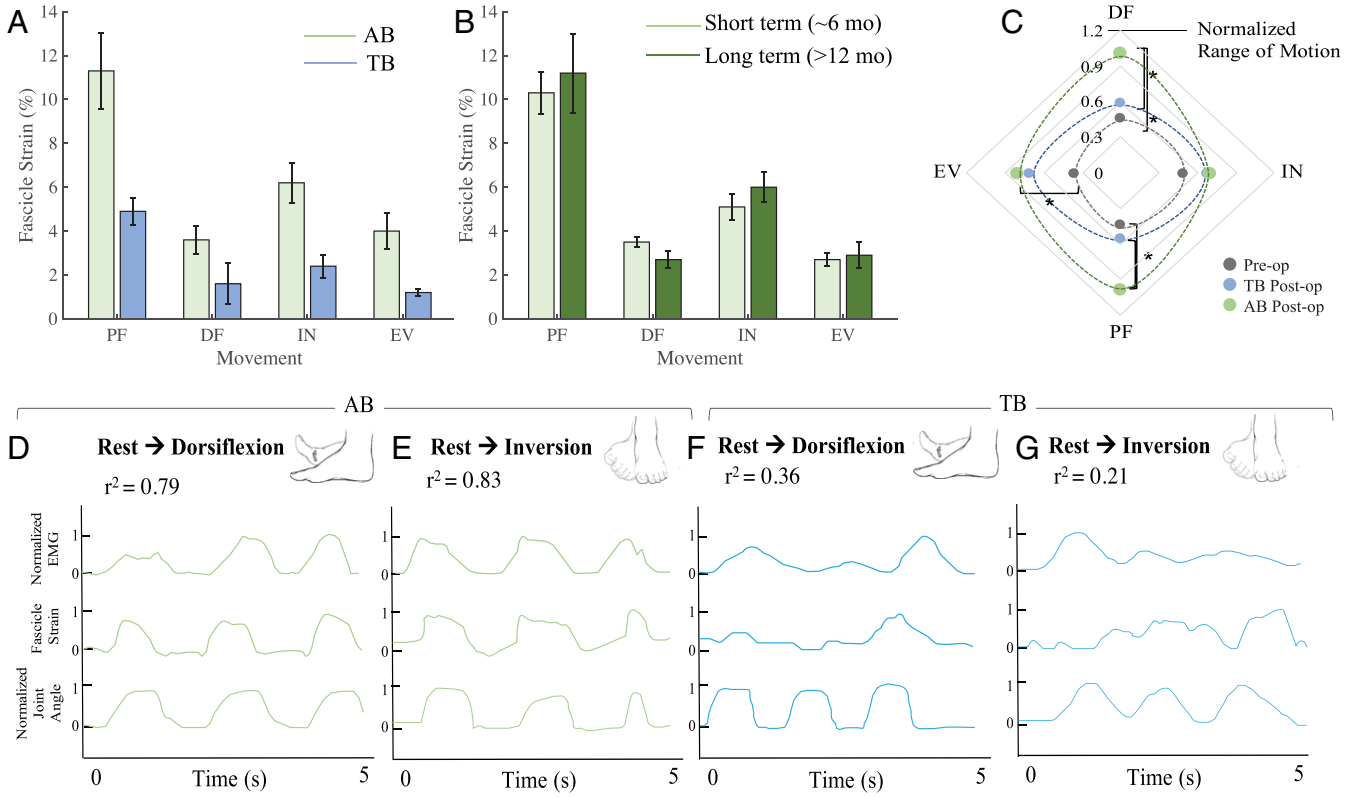

Fig. 2. Agonist–antagonist muscle coupling and ROM. (*A*) Mean and SD of fascicle strains of antagonist muscle during agonist muscle contraction during plantarflexion (PF), dorsiflexion (DF), inversion (IN), and eversion (EV) of the AB ($n = 14$, green) and TB ($n = 6$, blue) cohorts at the first testing session. (*B*) Average fascicle strains in the AB cohort at the first and second testing sessions (6 to 12 mo, light green; 12+ mo, dark green) ($n = 6$) after surgery. (*C*) ROM percepts for the subtalar and ankle joints. (*D*–*G*) The normalized EMG, normalized fascicle strain from the target muscle of the affected limb, and normalized joint angle of the unaffected limb are plotted from a representative subject to demonstrate the level of coupling in the residual limb muscles for the AB cohort (*D* and *E*) and the TB cohort (*F* and *G*). Temporal correlation of these data is represented by the r^2 values. In AB subjects (*D* and *E*), a high level of coupling is present in the AMI constructs. In TB subjects (*F* and *G*), there is relatively little coupling of the fascicle strain to the normalized EMG.

discrimination in every category except between 75% PF and 100% PF compared to TB subjects ($P < 0.05$, two-tailed t test, Fig. 3*C*). Variance between repetitions at each level was compared between cohorts using a repeated-measures F test, Bonferroni corrected for multiple comparisons at a statistical significance alpha of $P < 0.008$. AB subjects demonstrated significantly less variance while performing the task when compared to TB subjects. The P values for individual subjects' F tests are

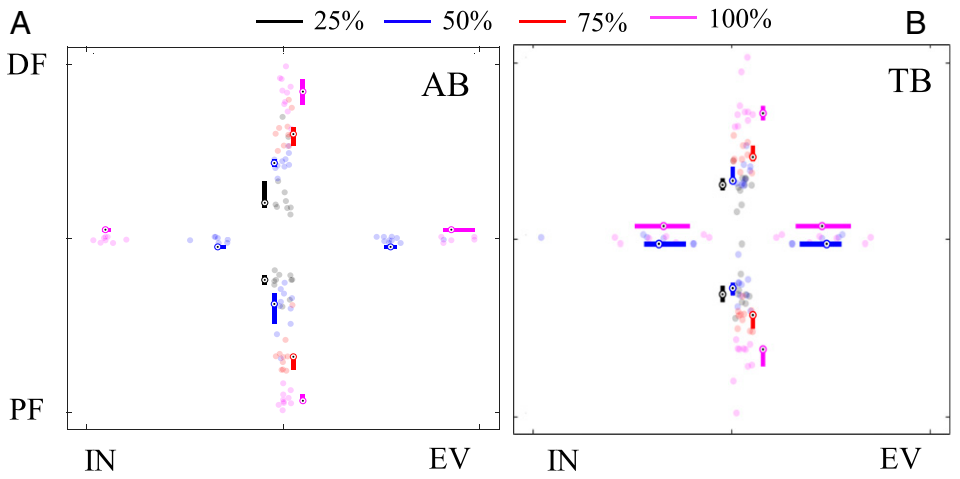

C

		P-value	
		AB	TB
PF	25-50	0.035	
	50-75	0.02	
	75-100		0.001
DF	25-50	0.03	
	50-75	0.01	
	75-100	0.01	
IN	50-100	0.03	
EV	50-100	0.01	

Fig. 3. (*A* and *B*) Positional differentiation capabilities for the median performer in the (*A*) AB cohort and (*B*) TB cohort according to their muscle activation. The mean and SD are represented by the bar and circle. Shaded data points show intrasubject repetitions for each commanded position (25%, black; 50%, blue; 75%, red; and 100%, pink). (*C*) P value for all significant comparisons of the difference between activation levels in adjacent categories (AB, $n = 14$; TB, $n = 6$) among all subjects.

presented in *SI Appendix*, Fig. S6. Together, these data demonstrate that AB subjects possess more precise and distinct motor control of their residual muscles, likely informed by greater proprioceptive input and enabling more distinct signal production for neuroprosthetic control.

Discussion

The AMI BKA procedure is designed to restore neuromuscular relationships, enabling proprioception and isolated EMG signal production toward improved prosthetic control. The present study characterizes physiological outcomes for the 15 subjects who had undergone an AMI BKA (AB cohort, $n = 15$), validating the resulting physiology and mechanistic effect of the AMI muscle dynamics on proprioception and related functions.

Overall, the data strongly supported our hypotheses and mechanistic basis of the AMI BKA. AMI muscles were found to be functioning with the designed agonist–antagonist dynamics, enabling active muscle excursion which gives rise to musculotendinous proprioceptive afferents. However, in TB subjects, given the isometric nature of the residual muscles and lack of agonist–antagonist coupling, the muscles' force oscillated periodically with continued invariance in strain. Such dynamics lead to incongruity between the intended and perceived motions, contributing to maladaptive central plasticity and uncoordinated residual muscle control (11, 12, 43). The roles of coupled muscle dynamics and proprioceptive feedback in guiding remodeling, motor imagery, and coordination were evident in the results of the motor task performance, self-reported metrics, and correlations thereof. Specifically, AB subjects reported healthy phantom sensations, greater phantom ROM percepts, and decreased pain compared to TB subjects, highlighting the potential for this procedure to promote enhanced neurological health of persons undergoing amputation.

Significantly greater fascicle strains were evinced in the residual muscles of AB subjects. Spindles fire at a rate proportional to muscle fiber length and thus, a greater strain in a given muscle enables more granular resolution of the musculotendinous afferents that are generated (44, 45). These were hypothesized to result in greater phantom percepts (phantom sensation and range of motion) and positively impact the production of EMG at different activation levels. In alignment with this neurophysiological principle, phantom sensation and range of motion percepts corelated to fascicle strains (*SI Appendix*, Fig. S5). Furthermore, performance on motor tasks demonstrated that AB subjects were capable of significantly greater positional differentiation and coordination of movements. Better performance in motor tasks, as seen in the present study, was likely facilitated by the higher quality and volume of musculotendinous afferent information from spindle fibers and Golgi tendon organs interacting with the central nervous system (46) as well as more coordinated motor activation in the peripheral neuromusculature (11). Neuroimaging in the brain areas associated with proprioception in patients with AMI amputation has demonstrated activation during a free space motor task at levels similar to those in control subjects, whereas they are significantly decreased in subjects with traditional amputation (46). Moreover, the degree of proprioceptive activity in the brain strongly correlated with fascicle activity in the peripheral muscles, further substantiating the mechanistic principle of the AMI.

These results have valuable implications on two fronts: 1) neurological health and 2) neuroprosthetic controllability. Liberation of the residual muscles aids in mitigating uncomfortable and unnatural perceptions of the phantom limb. This may contribute to greater utilization of standard prostheses, higher functional status, and less metabolic strain, given the comfort and improvement in the residual limb functionality. Further, the provision of proprioceptive pathways and preservation of lower motor neurons, via construction of AMIs, mitigate reorganization in subcortical and cortical structures of the brain that yield chronic pain and aberrant sensations and are responsible for normal sensorimotor processing (9, 24, 46). Increased coordination of intended phantom movements and muscle activation, involving preserved central sensorimotor functional connectivity (46), facilitates cleaner efferent motor signals for neural prostheses. With current amputation approaches, muscles are often haphazardly arranged and cocontract within the residuum due to scarring. Since the resulting EMG signals are hard to decode and translate to the intended movements, current prostheses heavily rely on pattern recognition approaches. In contrast, the AMI separates and allows dynamic sliding of muscles for each joint, resulting in high signal-to-noise ratio EMG signals for each intended movement. Moreover, the increase in proprioception enables a reduction in cocontraction and improved efferent signaling of proprioception-based reflexes, yielding improved control signals. Further, the independence of EMG signals produced for each desired activation level is a positive indicator for the viability and efficacy of direct neural control of prostheses, as opposed to pattern-recognition–based approaches. These suggest that AMI BKA subjects may be able to control myoelectric prostheses with greater fidelity than their traditional BKA counterparts.

While the AMI architecture mimics the reciprocal muscle relationships of a limb in free space, the force–displacement relationships will be modified under external loading. FES applied to the antagonist muscle will contribute to a sense of force feedback, although neural adaptation to the modified muscle dynamics may be required. A framework for the use of FES in such a manner was described in Clites et al. (11). Further studies focusing on FES to the antagonist muscle will provide greater insight into the role of force feedback from Golgi tendon organs and the adaptation of motor control by AMI muscles to more complex movements under loaded conditions. Ongoing surgical modifications incorporating osseointegration (1) and techniques from cineplasty (47) may also contribute to more advanced neuromuscular architectures. The proprioceptive mechanoneural interface (PMI) is a newer approach that couples each muscle end organ with a computer-controlled muscle actuator wherein the biological transmission that maps muscular linear movement to joint rotation is defined in software using an intact biophysical limb model (48). In this approach, external forces, such as inertia and gravitation, applied to the prosthesis or limb can be independently applied to the muscle end organ without antagonist end organ activation.

Limitations of the study include the mismatch in the population sizes that were studied. This investigation is ongoing and future reports will contain a larger set of data. Further, the AMI amputation could be studied in comparison to a cohort of subjects with TMR or RPNIs incorporated at amputation. Future exploration into the roles of rehabilitation and cutaneous feedback (22, 49, 50) may enhance the understanding of neurophysiology following amputation. A comparison of long-term outcomes in both groups and pre/postscores of PROMIS metrics would be valuable.

In conclusion, this investigation demonstrates that the construction of AMIs during amputation holds benefits for persons undergoing amputation, regardless of their prosthetic choice. As an added advantage, the AMIs restore proprioceptive circuits, boost motor imagery, and offer significantly differentiable surface EMG signals, all of which will improve myoelectric control.

Data Availability. All data are available in the main text or *SI Appendix*. Code for converting and visualizing the EMG data have been deposited in GitHub: https://github.com/shriyas133/AMI-amputation.

ACKNOWLEDGMENTS. This work was supported by 1) MIT Media Lab Consortia, 2) National Institute of Child Health and Human Development and National Center for Medical Rehabilitation Research of the National Institutes of Health Grant R01HD097135 associated with NCT03913273, and 3) Department of Defense Grant W81XWH16 PRORP-CTA OR160165A associated with NCT03374319. We are grateful to T. Clites, S.-H. Yeon, K. Clites, and L. Berger for experimental setup and help with research logistics. We defined our research questions and methodology based on input and conversations with patients. It was difficult to directly involve the public and patients in the other areas of the study design due to data protection restrictions and the very technical methods required for data analysis. We engage with amputee support groups and the public to disseminate the results through online, print, and in person media.

1. H. M. Herr *et al*., Reinventing extremity amputation in the era of functional limb restoration. *Ann. Surg.*, 10.1097/SLA.0000000000003895 (2020).
2. H. X. Qi, I. Stepniewska, J. H. Kaas, Reorganization of primary motor cortex in adult macaque monkeys with long-standing amputations. *J. Neurophysiol.* **84**, 2133–2147 (2000).
3. T. P. Pons *et al*., Massive cortical reorganization after sensory deafferentation in adult macaques. *Science* **252**, 1857–1860 (1991).
4. M. A. R. O'Reilly *et al*., Neuromas as the cause of pain in the residual limbs of amputees. An ultrasound study. *Clin. Radiol.* **71**, 1068.e1-6 (2016).
5. T. R. Makin *et al*., Phantom pain is associated with preserved structure and function in the former hand area. *Nat. Commun.* **4**, 1570 (2013).
6. H. Flor, L. Nikolajsen, T. Staehelin Jensen, Phantom limb pain: A case of maladaptive CNS plasticity? *Nat. Rev. Neurosci.* **7**, 873–881 (2006).
7. A. D. Houghton, G. Nicholls, A. L. Houghton, E. Saadah, L. McColl, Phantom pain: Natural history and association with rehabilitation. *Ann. R. Coll. Surg. Engl.* **76**, 22–25 (1994).
8. M. Pazzaglia, M. Zantedeschi, Plasticity and awareness of bodily distortion. *Neural Plast.* **2016**, 9834340 (2016).
9. K. L. Collins *et al*., A review of current theories and treatments for phantom limb pain. *J. Clin. Invest.* **128**, 2168–2176 (2018).
10. N. Sharma, P. S. Jones, T. A. Carpenter, J.-C. Baron, Mapping the involvement of BA 4a and 4p during motor imagery. *Neuroimage* **41**, 92–99 (2008).
11. T. R. Clites *et al*., Proprioception from a neurally controlled lower-extremity prosthesis. *Sci. Transl. Med.* **10**, eaap8373 (2018).
12. T. R. Clites, H. M. Herr, S. S. Srinivasan, A. N. Zorzos, M. J. Carty, The Ewing amputation: The first human implementation of the agonist-antagonist myoneural interface. *Plast. Reconstr. Surg. Glob. Open* **6**, e1997 (2018).
13. M. Seyedali, J. M. Czerniecki, D. C. Morgenroth, M. E. Hahn, Co-contraction patterns of trans-tibial amputee ankle and knee musculature during gait. *J. Neuroeng. Rehabil.* **9**, 29 (2012).
14. A. M. Smith, The coactivation of antagonist muscles. *Can. J. Physiol. Pharmacol.* **59**, 733–747 (1981).
15. A. W. Nelson, The painful neuroma: The regenerating axon versus the epineural sheath. *J. Surg. Res.* **23**, 215–221 (1977).
16. J. Wright, V. G. Macefield, A. van Schaik, J. C. Tapson, A review of control strategies in closed-loop neuroprosthetic systems. *Front. Neurosci.* **10**, 312 (2016).
17. A. W. Franzke *et al*., Users' and therapists' perceptions of myoelectric multi-function upper limb prostheses with conventional and pattern recognition control. *PLoS One* **14**, e0220899 (2019).
18. N. Parajuli *et al*., Real-time EMG based pattern recognition control for hand prostheses: A review on existing methods, challenges and future implementation. *Sensors (Basel)* **19**, 4596 (2019).
19. L. J. Hargrove, L. A. Miller, K. Turner, T. A. Kuiken, Myoelectric pattern recognition outperforms direct control for transhumeral amputees with targeted muscle reinnervation: A randomized clinical trial. *Sci. Rep.* **7**, 13840 (2017).
20. B. J. Brown *et al*., Outcomes after 294 transtibial amputations with the posterior myocutaneous flap. *Int. J. Low. Extrem. Wounds* **13**, 33–40 (2014).
21. R. L. Sainburg, M. F. Ghilardi, H. Poizner, C. Ghez, Control of limb dynamics in normal subjects and patients without proprioception. *J. Neurophysiol.* **73**, 820–835 (1995).
22. M. Schiefer, D. Tan, S. M. Sidek, D. J. Tyler, Sensory feedback by peripheral nerve stimulation improves task performance in individuals with upper limb loss using a myoelectric prosthesis. *J. Neural Eng.* **13**, 016001 (2016).
23. R. F. F. Weir, Extrapolation of emerging technologies and their long-term implications for myoelectric versus body-powered prostheses: An engineering perspective. *JPO J. Prosthet. Orthot.* **29**, P63–P74 (2017).
24. C. P. van der Schans, J. H. B. Geertzen, T. Schoppen, P. U. Dijkstra, Phantom pain and health-related quality of life in lower limb amputees. *J. Pain Symptom Manage.* **24**, 429–436 (2002).
25. M. Razmus, B. Daniluk, P. Markiewicz, Phantom limb phenomenon as an example of body image distortion. *Curr. Probl. Psychiatry* **18**, 153–159 (2017).
26. S. Ali, S. K. Fatima Haider, Psychological adjustment to amputation: Variations on the bases of sex, age and cause of limb loss. *J. Ayub Med. Coll. Abbottabad* **29**, 303–307 (2017).
27. X. Fuchs, R. Bekrater-Bodmann, H. Flor, "Phantom pain: The role of maladaptive plasticity and emotional and cognitive variables" in *Pain, Emotion and Cognition: A Complex Nexus*, G. Pickering, S. Gibson, Eds. (Springer International Publishing, 2015), pp. 189–207.
28. T. A. Kuiken *et al*., Targeted muscle reinnervation for real-time myoelectric control of multifunction artificial arms. *JAMA* **301**, 619–628 (2009).
29. J. M. Souza *et al*., Targeted muscle reinnervation: A novel approach to postamputation neuroma pain. *Clin. Orthop. Relat. Res.* **472**, 2984–2990 (2014).
30. C. A. Kubiak, S. W. P. Kemp, P. S. Cederna, T. A. Kung, Prophylactic regenerative peripheral nerve interfaces to prevent postamputation pain. *Plast. Reconstr. Surg.* **144**, 421e–430e (2019).
31. Z. T. Irwin *et al*., Chronic recording of hand prosthesis control signals via a regenerative peripheral nerve interface in a rhesus macaque. *J. Neural Eng.* **13**, 046007 (2016).
32. U. Proske, S. C. Gandevia, The proprioceptive senses: Their roles in signaling body shape, body position and movement, and muscle force. *Physiol. Rev.* **92**, 1651–1697 (2012).
33. H. M. Herr, R. R. Riso, K. W. Song, R. J. Casler Jr., M. J. Carty, "Peripheral neural interface via nerve regeneration to distal tissues." US Patent US20160346099 (2016).
34. H.M. Herr *et al*., "Method and System for Providing Proprioceptive Feedback and Functionality Mitigating Limb Pathology." US Patent US20190021883 (2019).
35. T. R. Clites, M. Carty, S. Srinivasan, A. Zorzos, H. Herr, A murine model of a novel surgical architecture for proprioceptive muscle feedback and its potential application to control of advanced limb prostheses. *J. Neural Eng.* **14**, 036002 (2017).
36. S. S. Srinivasan *et al*., On prosthetic control: A regenerative agonist-antagonist myoneural interface. *Sci. Robot.* **2**, eaan2971 (2017).
37. S. S. Srinivasan, M. Diaz, M. Carty, H. M. Herr, Towards functional restoration for persons with limb amputation: A dual-stage implementation of regenerative agonist-antagonist myoneural interfaces. *Sci. Rep.* **9**, 1981 (2019).
38. I. L. Valerio *et al*., Preemptive treatment of phantom and residual limb pain with targeted muscle reinnervation at the time of major limb amputation. *J. Am. Coll. Surg.* **228**, 217–226 (2019).
39. C. W. Ertl, J. P. Ertl, W. J. J. Ertl, "The Ertl osteomyoplastic amputation." *The Academy Today* **6**, A-5–A-8 (2010).
40. B. C. Taylor, A. Poka, Osteomyoplastic transtibial amputation: The Ertl technique. *J. Am. Acad. Orthop. Surg.* **24**, 259–265 (2016).
41. Northwestern University, PROMIS scoring manuals. https://www.healthmeasures.net/promis-scoring-manuals. Accessed 24 May 2020.
42. D. J. Farris, G. A. Lichtwark, UltraTrack: Software for semi-automated tracking of muscle fascicles in sequences of B-mode ultrasound images. *Comput. Methods Programs Biomed.* **128**, 111–118 (2016).
43. C. R. Claret *et al*., Neuromuscular adaptations and sensorimotor integration following a unilateral transfemoral amputation. *J. Neuroeng. Rehabil.* **16**, 115 (2019).
44. V. G. Macefield, T. P. Knellwolf, Functional properties of human muscle spindles. *J. Neurophysiol.* **120**, 452–467 (2018).
45. D. M. Lewis, U. Proske, The effect of muscle length and rate of fusimotor stimulation on the frequency of discharge in primary endings from muscle spindles in the cat. *J. Physiol.* **222**, 511–535 (1972).
46. S. S. Srinivasan *et al*., Agonist-antagonist myoneural interface amputation preserves proprioceptive sensorimotor neurophysiology in lower limbs. *Sci. Transl. Med.* **12**, eabc5926 (2020).
47. R. F. Weir, C. W. Heckathorne, D. S. Childress, Cineplasty as a control input for externally powered prosthetic components. *J. Rehabil. Res. Dev.* **38**, 357–363 (2001).
48. H. Herr, H. Song, S. Srinivasan, "Mechanoneural interfaces for prosthetic control." US patent application no. 63/029,137 (2020).
49. J. S. Hebert *et al*., Novel targeted sensory reinnervation technique to restore functional hand sensation after transhumeral amputation. *IEEE Trans. Neural Syst. Rehabil. Eng.* **22**, 765–773 (2014).
50. S. Srinivasan, H. Herr, A cutaneous mechanoneural interface for neuroprosthetic feedback. *Nat. Biomed. Eng.*, 10.1038/s41551-020-00669-7 (2020).